

# A ROBUST WATERMARKING SCHEME BASED ON EDGE DETECTION AND CONTRAST SENSITIVITY FUNCTION

John N. Ellinas

*Department of Electronic Computer Systems, Technological Education Institute of Piraeus, 12244 Egaleo, Greece*

Dimitrios E. Manolakis

*Department of Automation, Alexander Technological Education Institute of Thessaloniki, 57400 Thessaloniki, Greece*

**Keywords:** Image watermarking, wavelet transform, Human Visual System, Contrast Sensitivity Function.

**Abstract:** The efficiency of an image watermarking technique depends on the preservation of visually significant information. This is attained by embedding the watermark transparently with the maximum possible strength. The current paper presents an approach for still image digital watermarking in which the watermark embedding process employs the wavelet transform and incorporates Human Visual System (HVS) characteristics. The sensitivity of a human observer to contrast with respect to spatial frequency is described by the Contrast Sensitivity Function (CSF). The strength of the watermark within the decomposition subbands, which occupy an interval on the spatial frequencies, is adjusted according to this sensitivity. Moreover, the watermark embedding process is carried over the subband coefficients that lie on edges where distortions are less noticeable. The experimental evaluation of the proposed method shows very good results in terms of robustness and transparency.

## 1 INTRODUCTION

The rapid evolution of multimedia systems and the wide distribution of digital data over the World Wide Web addresses the copyright protection of digital information. The aim is to embed copyright information, which is called watermark, on digital data (audio or visual) in order to protect ownership. In general, a digital watermarking technique must satisfy two requirements. First, the watermark should be transparent or perceptually invisible for image data. The second requirement is that the watermark should be resistant to attacks that may remove it or replace it with another watermark. This implies that the watermark should be robust to common signal processing operations, such as compression, filtering, enhancements, rotation, cropping and translation.

The digital image watermarking techniques in the literature are typically grouped in two classes: the spatial domain techniques (Schyndel et al., 1994; Bender et al., 1996; Wolfgang and Delp, 1996) which embed the watermark by modifying the pixel

values of the original image and the transform domain techniques which embed the watermark in the domain of an invertible transform. The discrete cosine transform (DCT) and the discrete wavelet transform (DWT) are commonly used for watermarking purposes (Swanson et al., 1996; Cox et al., 1997; Xia et al., 1997; Kim and Moon, 1997; Dugad et al., 1998; Hsu and Wu, 1999; Wolfgang et al., 1999; Barni et al., 2001). The transform domain algorithms modify a subset of the transform coefficients with the watermarking data and generally achieve better robustness than spatial domain methods. Optionally, they may employ a human visual perception model to weight the strength of the embedded data. Several research works employ the wavelet transform because it presents a number of advantages over the DCT. The wavelet transform is closer to the human visual system since it splits the input image into several frequency bands that can be processed independently. It is a multi-resolution transform that permits to locate image features such as smooth areas, edges or textured areas. Some watermarking schemes embed watermarking data in textured areas

N. Ellinas J. and E. Manolakis D. (2007).

A ROBUST WATERMARKING SCHEME BASED ON EDGE DETECTION AND CONTRAST SENSITIVITY FUNCTION.

In *Proceedings of the Second International Conference on Computer Vision Theory and Applications - ICFIA*, pages 93-100

Copyright © SciTePress

or edges where human visual system (HVS) is less sensitive. Many HVS models have been developed for quality assessment or image compression (De Vleeschouwer et al., 2002). Similar visual models are employed for digital watermarking with a great success. One model for perceptual watermarking exploits the contrast sensitivity of the human eye over the spatial frequency, which is described by the contrast sensitivity function (CSF), in order to weight the coefficients of a transform domain.

In this paper, an additive watermarking algorithm embeds the signature data to selected groups of wavelet transform coefficients, weighting the watermark strength according to the CSF sensitivity of the subband where the corresponding coefficients reside. The input image is decomposed into four levels by a DWT, an approximation subband including the low frequency components and 12 detail subbands including the high frequency components. Every subband occupies a specific spatial frequency interval that corresponds to an average contrast sensitivity factor which is the weight of the watermark strength. Moreover, the proposed algorithm detects edges in each subband and distributes the watermark energy in these regions, where HVS is less sensitive to. Finally, the receiver detects the signature data by correlating the watermarked image with the watermark sequence and comparing the correlation factor to a threshold value. The motivation of the present work is to adapt a watermark sequence to the local image properties by employing a visual model, providing a transparent and robust watermark.

## 2 CSF CHARACTERISTICS

The characteristics of the contrast sensitivity function in HVS model may be applied on the coefficients of the detail subbands in the wavelet decomposition of an image.

### 2.1 The Contrast Sensitivity Function

Based on the research of the human visual system, several mathematical models have been devised to characterize humans' sensitivity to brightness and color (Wandell, 1995). The contrast sensitivity function describes humans' sensitivity to spatial frequencies. A model of the CSF for luminance (or grayscale) images, originally proposed by Mannos and Sakrison (Mannos and Sakrison, 1994), is given by:

$$CSF(f) = 2.6(0.192 + 0.114f)e^{-(0.114f)^{1.1}} \quad (1)$$

Fig. 1 illustrates the CSF curve which characterizes the luminance sensitivity of HVS with respect to spatial frequency. According to this curve, HVS is less sensitive at very low and very high frequencies. The properties of CSF may be used to weight the watermark embedded data so that to be transparent for a human observer.

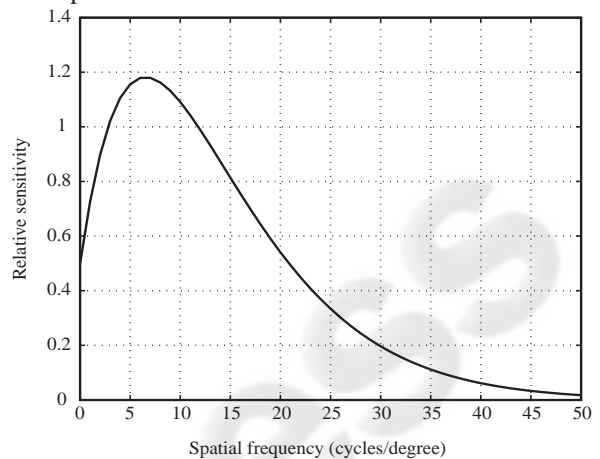


Figure 1: Luminance contrast sensitivity function.

### 2.2 CSF Weighting in DWT Domain

The DWT decomposes a two dimensional image into subbands using low and high pass filters for the rows and columns successively. The edge components of the image are confined within the high frequency part (detail subbands) whereas the low frequency part (approximation subband) splits again until reaching the desired resolution.

Fig.2 shows a four level wavelet decomposition where each subband is covered by a specific spatial frequency range. For example, subband HL3 of level  $l=3$  and orientation  $\theta=1$ , which describes the vertical details by indicating the luminance variations along the horizontal direction, is covered by horizontal frequencies from  $0.125f_{max}$  to  $0.25f_{max}$  and vertical frequencies from 0 to  $0.125f_{max}$ . The area of the CSF along the horizontal and vertical directions that corresponds to the spatial frequency range covered by this subband is shaded. Therefore, the weighting for the coefficients of the specific subband must be estimated by the shaded portions of the CSF function.

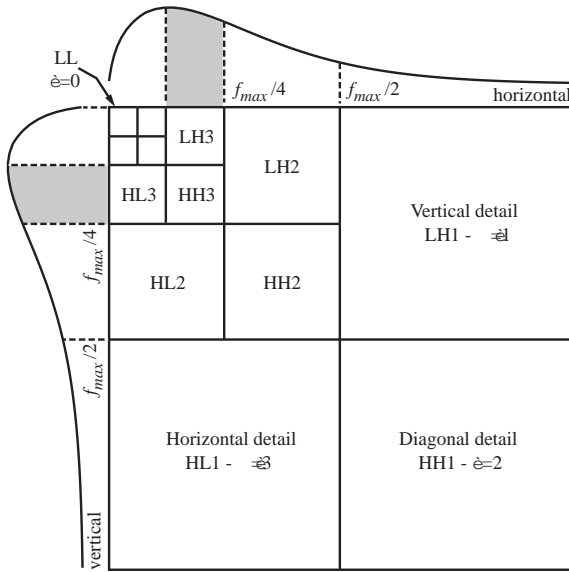


Figure 2: Luminance CSF along horizontal and vertical directions of four level wavelet decomposition.

### 3 CSF BASED WATERMARKING

The CSF exploitation in the watermarking process is accomplished by weighting the coefficients of the wavelet transform according to the subband they belong to. The additive embedding algorithm and its detection at the receiver's end are analyzed as follows:

#### 3.1 The Watermark Embedding Process

Fig. 3 shows the overall process of watermark insertion. The input image is subjected to a four level DWT decomposition using the Daubechies 8-tap filter.

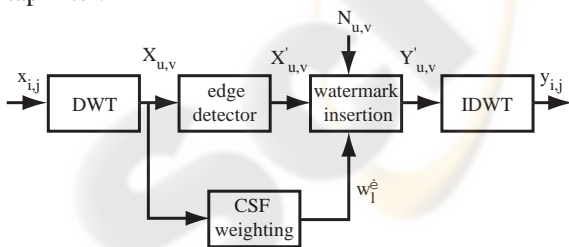


Figure 3: Block diagram of the watermark insertion process.

The perceptually important wavelet coefficients of each subband are detected by Sobel edge detector.

To the selected coefficients, the watermark is inserted in an additive way using (2). The detail subbands, where the watermark is inserted, contain edge information or high frequency coefficients. Consequently, adding the watermark to these coefficients makes the insertion invisible to the human visual system. Moreover, the insertion is weighted according to the sensitivity of the human visual system to the contrast, which depends on the spatial frequency.

$$Y'_{u,v} = X'_{u,v} + \alpha_l w_l^\theta X'_{u,v} N_{u,v} \quad (2)$$

where  $Y'_{u,v}$  are the modified wavelet coefficients,  $X'_{u,v}$  are the edge selected wavelet coefficients,  $\alpha_l$  is a level dependent parameter controlling the watermark strength,  $w_l^\theta$  is the subband visual weight at level  $l$  and orientation  $\theta$ , and  $N_{u,v}$  is the watermark sequence which is represented by Gaussian noise with zero mean and unit variance.

Fig. 4 illustrates the perceptually significant wavelet coefficients of the vertical detail subband at level 2 for "Lena". The visual weighting factors for each subband are estimated by averaging the portion of the CSF curve that corresponds to the high spatial frequency part. The magnitude of the watermark strength scale factor is selected for each level of the wavelet decomposition such that not severely degrading the watermarked image quality and considering the fact that the average magnitude of the coefficients is approximately doubled in each level from the finest to the coarsest resolution.



Figure 4: Edge coefficients of the vertical orientation subband at level 2.

### 3.2 The Watermark Detection Process

The possibly distorted watermark sequence is detected by combining the original image  $x$  with the possibly distorted watermarked image  $y^*$  reversing the steps of the insertion process, as Fig. 5 shows.

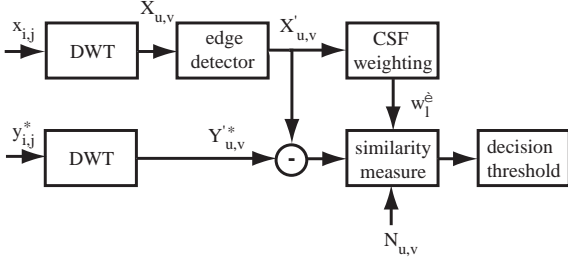


Figure 5: Block diagram of the watermark detection process.

The extraction process is performed by subtracting the original perceptual significant coefficients from the corresponding received watermarked coefficients (which may have been attacked and distorted) and scaling the difference by the weighting and watermark strength factors. The watermark detection is accomplished without referring to the original image, considering the correlation between the watermarked coefficients and the watermarking sequence (Barni et al., 2001):

$$\rho = \frac{1}{MN} \sum_{u=0}^{M-1} \sum_{v=0}^{N-1} Y_{u,v}' N_{u,v} \quad (3)$$

where  $Y_{u,v}'$  represents the watermarked perceptually significant coefficients and  $N_{u,v}$  is the watermark sequence.

The correlation factor is compared to a threshold value, as in (4)

$$\begin{aligned} \rho > T_w & \text{ true watermark} \\ \rho < T_w & \text{ false watermark} \end{aligned} \quad (4)$$

where

$$T_w = 3.97\sqrt{2\sigma^2} \quad (5)$$

Variance  $\sigma$  is defined as

$$\sigma = \frac{1}{(MN)^2} \sum_{u=0}^{M-1} \sum_{v=0}^{N-1} (Y_{u,v}')^2 \quad (6)$$

### 3.3 Image Quality Assessment

The objective evaluation of image quality is performed by the PSNR, which is defined as

$$PSNR = 10 \log_{10} \left( \frac{255 \times 255}{mse} \right) \quad (7)$$

where  $mse$  is the mean square error:

$$mse = \frac{1}{MN} \sum_{i=0}^{M-1} \sum_{j=0}^{N-1} [x(i,j) - y(i,j)]^2 \quad (8)$$

where  $M, N$  are the dimensions of the input image and  $x, y$  are the original and the watermarked images.

However, PSNR declines from the perceived subjective quality because the HVS does not correlate well with the square of the error. For this reason, the weighted PSNR that takes into account the local variance is also used as follows:

$$wPSNR = 10 \log_{10} \left( \frac{255 \times 255}{wmse} \right) \quad (9)$$

where

$$wmse = \frac{1}{MN} \sum_{i=0}^{M-1} \sum_{j=0}^{N-1} \left[ \frac{x(i,j) - y(i,j)}{1 + \text{var}(i,j)} \right]^2 \quad (10)$$

## 4 EXPERIMENTAL RESULTS

The proposed method is evaluated in four images: "Lena", which is an image with large smooth regions, "Barbara", "Baboon" and "Boat", which have textured regions. The size of all images is  $512 \times 512$  pixels. The performance measures are the invisibility of the inserted watermark and the robustness of the method against various types of attacks. The attacks employed for testing are JPEG compression, median filtering, Gaussian noise and cropping.



Figure 6: (a) Original image; (b) Watermarked image.

Fig. 6 shows the original image of “Lena” and its watermarked copy whereas Fig. 7 shows their difference. It is obvious that the watermarked copy is undistinguishable from the original image. In the difference, which is suitably scaled for display, it is evident that most of the watermark data are added to the edges where they are perceptually invisible.



Figure 7: Scaled difference between original and watermarked images.

Table 1 depicts the objective quality values of the proposed method for the tested images. These values are obtained setting the watermark strength factor to a low value so that the detector response is just over the threshold value. It is well known that the two desirable features of watermarking, invisibility and robustness, are contradictory. Thus, the values of the watermark strength factor  $\alpha_1$  are properly tuned so that the watermarking sequence is completely invisible although robustness is at a medium level. Fig. 8 shows the response of the watermark detector to 1000 randomly generated watermarks, with the original watermark placed in the middle. In this case, the watermark strength is such that the watermark sequence is robust enough

and the objective quality of the watermarked image is just above 35 dB, which is a typical value just before image is degrading.

Table 1: PSNR and wPSNR values of watermarked test images.

Images	PSNR (dB)	wPSNR (dB)
Lena	45.18	65.66
Barbara	44	64.21
Baboon	42.65	61.95
Boat	44.45	63.67

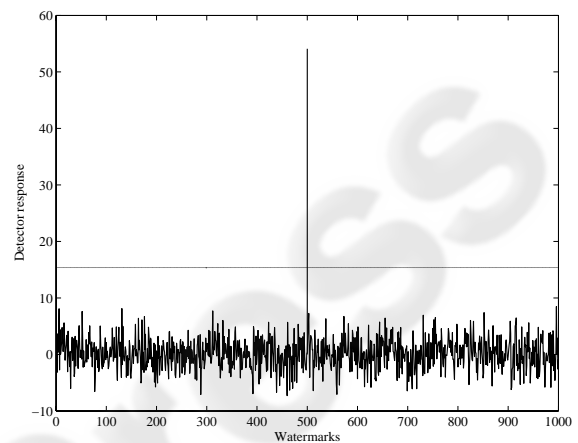


Figure 8: Response of watermark detector for “Lena”.

Table 2 shows the effectiveness of the proposed scheme against two other typical algorithms on wavelet-based watermarking (Dugad et al., 1998; Kim and Moon, 1999). The first method employs a unique threshold value over all the detail subbands for embedding the signature data, whereas the second method uses level adaptive thresholding for more accurate estimation of edge coefficients.

Table 2: PSNR and detector response values of three watermarking schemes for the test image “Lena”.

Algorithms	PSNR (dB)	Detector response
Proposed	35.11	<b>53.76</b>
Dugad et al.	35.73	28.20
Kim and Moon	35.18	43.60

The proposed scheme outperforms significantly over the other two methods for about the same objective quality of the watermarked image. This robust performance lies on the fact that watermark data are placed exactly on the detected edges where HVS is less sensitive to distortions. The threshold values employed by the other algorithms can not

exactly locate the edges on the wavelet domain and for that reason some watermark data are placed on coefficients that affect the quality of the image. Moreover, in the proposed method there are no threshold values that are image dependent and their tuning to optimum values is a serious drawback.

To appreciate the robustness of the proposed method against several common attacks, the following experiments were performed in “Lena” image.

Firstly, JPEG coding with variable quality factor was applied to the watermarked image and 1000 watermarks were inserted for examining the detector’s response about their presence. In Fig. 9, the response of the detector to the embedded watermark is plotted against the JPEG quality factor. Also, the detection threshold and the second highest response are shown. The detector response remains above threshold up to a quality factor of 5 whereas the second highest response remains always under the threshold value. This proves the robustness of the proposed method against JPEG compression.

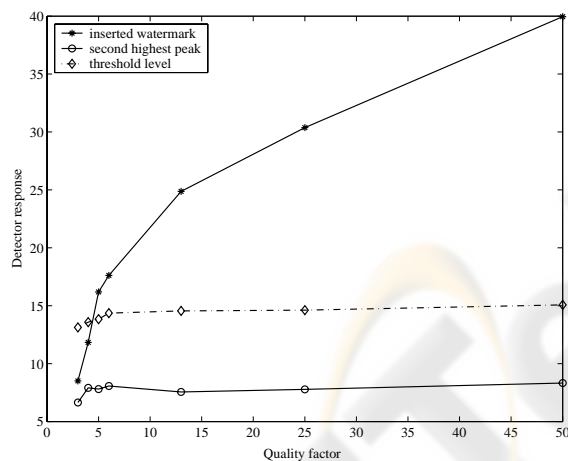


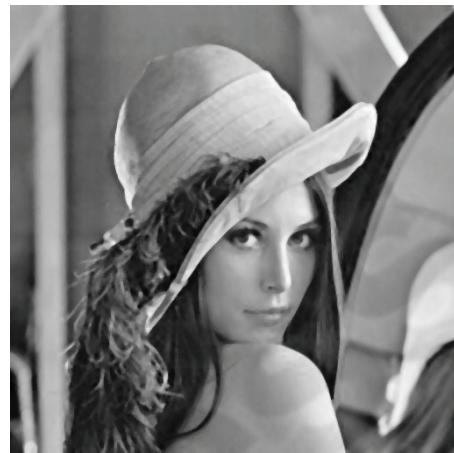
Figure 9: Detector response versus JPEG quality factor.

Fig. 10(a) illustrates the watermarked image after median filtering with a window size of  $3 \times 3$  whereas Fig. 10(b) shows the detector response to this kind of attack. Comparing this figure with Fig. 8, we observe that correlation factor decreases to about one third of its initial value because of median filtering. This may be explained since median filtering smoothes the edges of an image where nearly all of the watermarking data have been embedded.

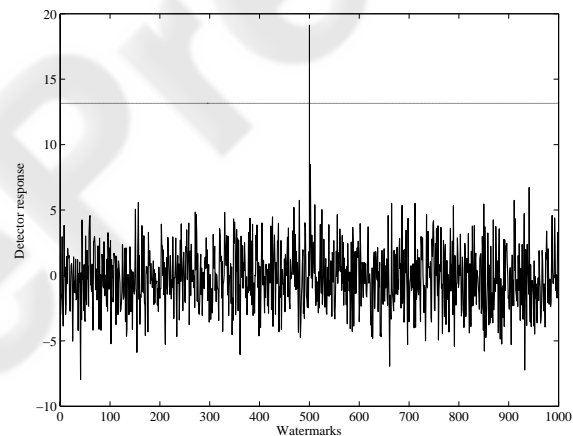
The proposed method is quite immune to Gaussian noise, as Fig. 11 shows. Fig. 11(a) presents the watermarked copy which has been contaminated with Gaussian noise of zero mean and variance of 20

whereas Fig. 11(b) shows the detector response. The output of the detector is slightly lower than that of Fig. 8, where no attack is involved.

Finally, the robustness of the proposed watermarking method against cropping is examined. When the watermarked image is cropped, part of the embedded information is discarded making the detection more elaborate.



(a)



(b)

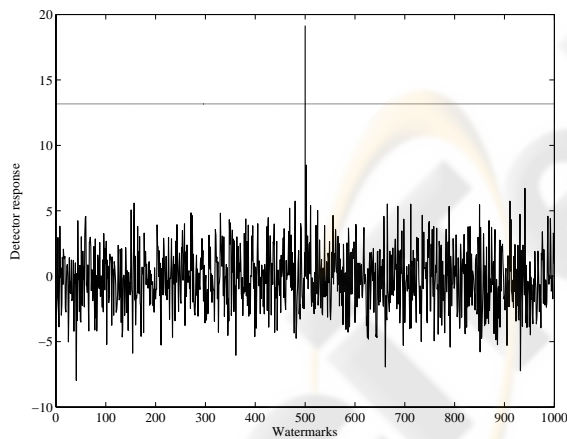
Figure 10: (a) Watermarked copy after median filtering; (b) Detector response of the attacked watermarked image.

Thus, it is important the watermark method to spread the information all over the image so that, if possible, any remaining part to include enough information for the watermark recovery. Our experiment on cropping is to examine the resilience of the watermark after the removal of a substantial part of the original image. Fig. 12(a) shows the cropped watermarked image which is half of the original image. The ability of the decoder to trace the watermark of the sub-image is shown in Fig.

12(b). It is quite impressive that the detector response is well above threshold, revealing the robustness of the proposed method. The watermark sequence is hidden on the wavelet coefficients that reside on the detail subbands or on the edges which exist all over the input image. The proposed method may be less effective when the remaining part contains mainly smooth areas where the embedded information is less, but this is difficult to be accomplished.

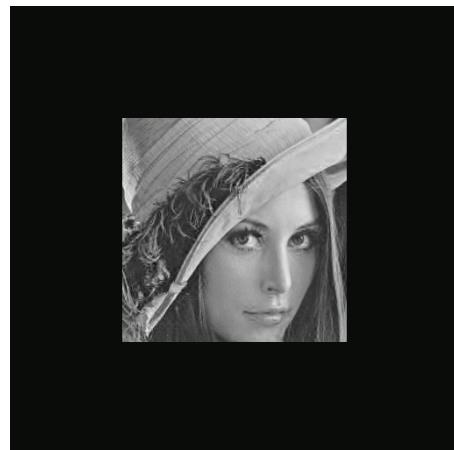


(a)

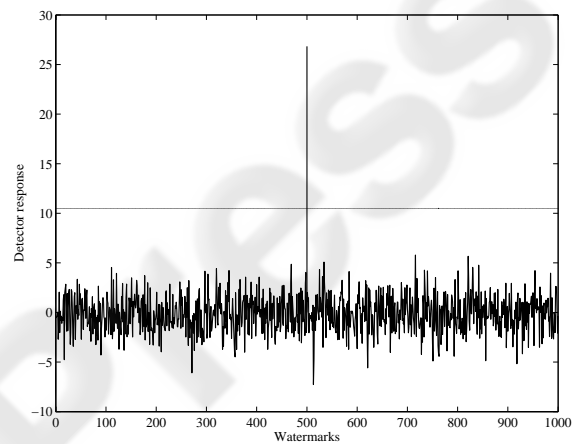


(b)

Figure 11: (a) Watermarked copy after Gaussian noise; (b) Detector response of the attacked watermarked image.



(a)



(b)

Figure 12: (a) Cropped watermarked copy; (b) Detector response of the cropped watermarked image.

## 5 CONCLUSIONS

In this paper, a novel method for image watermarking has been presented. The method embeds the watermarking data on selected wavelet coefficients of the input image considering the CSF characteristics of the HVS. The selected coefficients reside on the detail subbands and describe the edges of the image. Thus, exploiting the HVS which is less sensitive to alterations on high frequencies, the embedded information becomes invisible. The evaluation of the proposed method shows very good performance as far as invisibility and robustness is concerned. The proposed scheme behaves very well in various common signal processing methods as compression, filtering, noise and cropping.

## ACKNOWLEDGEMENTS

The project is co-funded by the European Social Fund and National Resources-EPEAEK II-ARCHIMEDES granted to Technological Education Institute of Thessaloniki under program number 10.

## REFERENCES

- Schyndel, R., Tirkel, A. and Osborne, C., 1994. A digital watermark. In *IEEE Proc. of International Conference on Image Processing 1994*.
- Bender, W., Gruhl, D., Morimoto, N. and Lu, A., 1996. Techniques for data hiding. In *IBM Systems Journal*, 35(3-4).
- Wolfgang, R. B. and Delp, E. J., 1996. A watermark for digital images," In *IEEE Proc. of International Conference on Image Processing 1996*.
- Swanson, M. D., Zhu, B. and Tewfik, A. H., 1996. Transparent robust image watermarking. In *IEEE Proc. of International Conference on Image Processing 1996*.
- Cox, I. J., Kilian, J., Leighton, T. and Shamoon, T., 1997. Secure spread spectrum watermarking for multimedia. In *IEEE Transactions on Image Processing*, 6(12).
- Barni, M., Bartolini, F. and Piva, A., 2001. Improved wavelet-based watermarking through pixel-wise masking. In *IEEE Transactions on Image Processing*, 10(5).
- Xia, X., Boncelet, C. G. and Arce, G. R., 1997. A multiresolution watermark for digital images. In *IEEE Proc. of International Conference on Image Processing 1997*.
- Kim, J. R. and Moon, Y. S., 1999. A robust wavelet-based digital watermarking using level-adaptive thresholding. In *IEEE Proc. of International Conference on Image Processing 1999*.
- Hsu, C. T. and Wu, J. L., 1999. Hidden digital watermarks in images. In *IEEE Transactions on Image Processing*, 8(1).
- Dugad, R., Ratakonda, K. and Ahuja, N., 1998. A new wavelet-based scheme for watermarking images. In *IEEE Proc. of International Conference on Image Processing 1998*.
- Wolfgang, R. B., Podilchuk, C. I. and Delp, E. J., 1999. Perceptual watermarks for digital images and video. In *SPIE Proc. of International Conference on Security and watermarking of multimedia contents 1999*.
- De Vleeschouwer, C., Delaigle, J. F. and Macq, B., 2002. Invisibility and application functionalities in perceptual watermarking an overview. In *IEEE Proc.*, 90(1).
- Wandell, B. A., 1995. *Foundations of Vision*, Sinauer Associates Inc., Sunderland MA.
- Mannos, J. and Sakrison, D., 1974. The effects of a visual fidelity criterion on the encoding of images. In *IEEE Transactions on Information Theory*, 20.